Local Spectrum-Trend Similarity Approach for Detecting Land-Cover Change by Using SPOT-5 Satellite Images

Penglin Zhang, Zhiyong Lv, and Wenzhong Shi

***Abstract*—Spectra-based change detection (CD) methods, such as image difference method and change vector analysis, have been widely used for land-cover CD using remote sensing data. However, the spectra-based approach suffers from a strict requirement of radiometric consistency in the multitemporal images. This letter proposes a new image feature named spectrum trend, which is explored from the spectral values of the image in a local geographic area (e.g., a 3 × 3 sliding window) through raster encoding and curve fitting techniques. The piecewise similarity between the paired local areas in the multitemporal images is calculated by using a sliding window centered at the pixel to generate the change magnitude image. Finally, CD is achieved by a threshold decision or a classified method. This proposed approach, called "local spectrum-trend similarity," is applied and validated by a case study of land-cover CD in Wuqin District, Tianjin City, China, by using SPOT-5 satellite images. Accuracies of "change" versus "no-change" detection are assessed. Experimental results confirm the feasibility and adaptability of the proposed approach in land-cover CD.**

***Index Terms*—Change detection (CD), land cover, local spectrum-trend similarity (LSTS), remote sensing image.**

I. Introduction

CHANGE detection (CD) is the process of identifying the difference in the state of an object or phenomenon by observing the object or phenomenon at different times [1]. Given the importance of monitoring the changes in the Earth surface, CD techniques have been an active topic, particularly in the field of land cover [2], [3]. In recent years, an increasing trend in the development of CD techniques by using remote sensing data has existed [4], [5]. The urgent task in remote sensing involves detection of land-cover change from a large amount of satellite data, which provide a valuable source of information for decision making processes [6], assessment of ecological health [7], and forest protection [8].

A variety of CD approaches for land cover have been reported, applied, and evaluated in land-cover binary CD, e.g., image difference [1] and background subtraction [9]. These algorithms, which are called "algebra CD," measure the change magnitude in a pixel-by-pixel manner by using algebraic operations in a straightforward manner. Thresholds are often necessary for dividing the change magnitude image into binary CD maps. Aside from the methods presented in [10]–[12], change vector analysis (CVA) and its derivatives are other examples of well-known CD techniques used widely in land cover. CVA is a spectral change-based approach that can process any number of spectral bands; therefore, CVA depends strongly on spectral information. Similar to raw image differencing, the CVA method is sensitive to the radiometric differences between multitemporal images. Fortunately, spectral correlation has been identified to overcome radiometric and dynamic range differences in land-cover CD [13]. Celik proposed a CD technique based on principal component analysis (PCA) and k-means [14]. The difference image is partitioned into $h \times h$ nonoverlapping blocks, and eigenvectors are extracted by PCA to create an eigenvector space. The CD is achieved by partitioning the feature vector space into two clusters using k-means clustering with $k = 2$. The Markov random field (MRF) is another widely used neighborhood-correlation-based CD approach. MRF provides a methodological framework for many scientific problems and energy minimization in image analysis [15]. Some studies analyze the difference image by using the MRF approach, which exploits the interpixel class dependence in the spatial domain to improve the accuracy of the binary CD result [16], [17]. Unlike the approach in [12], the labeled difference image by MRF is repeated iteratively until the energy function reaches convergence under a specified conditional distribution. Different CD algorithms have their own merits, and no single approach is optimal and applicable to all cases [6]. Review articles on CD using remote sensing images were reported to summarize and compare these CD techniques [1], [6]. Mas compared six CD techniques in monitoring land-cover change [18] and tested and compared 11 different binary CD methods in terms of their capability in detecting land-cover change or no-change information in different seasons [19].

Based on the aforementioned work, a novel approach called "local spectrum-trend similarity (LSTS)" is proposed in this letter. LSTS is used instead of the actual spectral value by a new exploring feature (spectrum trend) to smooth the performance of the pixels in a local area of the multitemporal images. LSTS transforms the actual spectral values within a sliding window into their corresponding spectrum. A curve fitting technique and a trend-similarity calculation approach were employed to measure the magnitude change between two date images in a local geographic area. In addition, two methods were evaluated to partition the change magnitude image into binary CD maps on the basis of the LSTS.

Manuscript received July 8, 2013; revised July 24, 2013; accepted August 6, 2013. Date of publication September 20, 2013; date of current version December 2, 2013. This work was supported by the High Technology Program of China under Grant 2012BAJ15B04.

P. Zhang and Z. Lv are with the School of Remote Sensing and Information Engineering, Wuhan University, Wuhan 430079, China.

W. Shi is with the Joint Spatial Information Research Laboratory between the Hong Kong Polytechnic University and Wuhan University, Kowloon, Hong Kong (e-mail: john.wz.shi@polyu.edu.hk).

Color versions of one or more of the figures in this paper are available online at http://ieeexplore.ieee.org.

Digital Object Identifier 10.1109/LGRS.2013.2278205

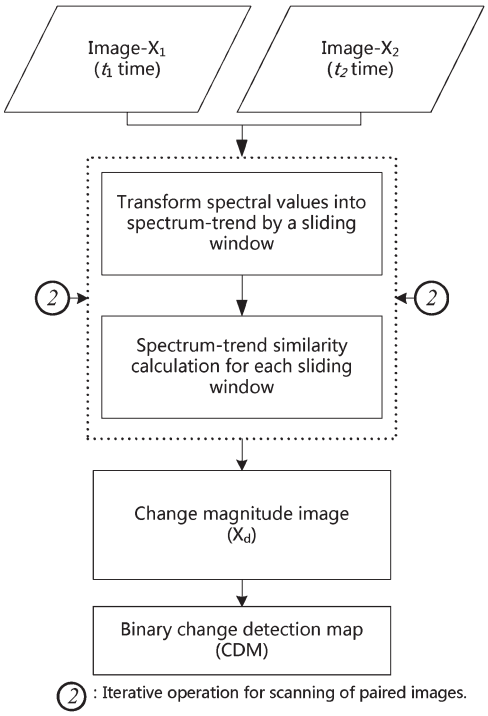

Fig. 1. General scheme of the proposed LSTS approach.

This letter is organized as follows: Section II describes the proposed CD approach, Section III tests the validity of the proposed approach by utilizing an actual case study and presents the experimental results, and Section IV reports the discussions and conclusion.

II. Methodology

Let $X_1 = \{x_1(i,j)|1 \le i \le W, 1 \le j \le H\}$ and $X_2 = \{x_2(i,j)|1 \le i \le W, 1 \le j \le H\}$ be the two coregistered images [size: $(W+1) \times (H+1)$] acquired on the same geographical area at different dates. The main objective of this work is to generate a binary CD map $\text{CDM} = \{\text{cdm}(i,j)|1 \le i \le W, 1 \le j \le H\}$, where $\text{cdm}(i,j) \in \{0, 255\}$. Fig. 1 shows the general scheme of the LSTS approach for binary CD. First, real spectral values within a specified window were transformed into the spectrum trend. Second, spectrum-trend similarity was calculated to generate the change magnitude image. Finally, a binary CD map was provided by a threshold or a classifier. The detailed processes of these steps will be discussed in the following sections.

A. Definition of Spectrum Trend

Trend is often evaluated in mining time series data [20], [21]. In our study, spectrum is a function of the reflectance spectral values within a specified window. If N is the total number of pixels within the window $x \in [0, N]$, let $f(x)$ be the function that can be estimated by generalized least squares (GLS) fitting technique from a discrete data set. The definition of spectrum trend for $f(x)$ can be given as a vector

$$T = (f'(t_1), f'(t_2), f'(t_3), \ldots, f'(t_m)) \tag{1}$$

where $t_m = m \times (N/k)$ and k is a descriptive coefficient of T. The larger the value of k is, the more detailed the trend of $f(x)$ described by T is. The value of k is usually no less than that of

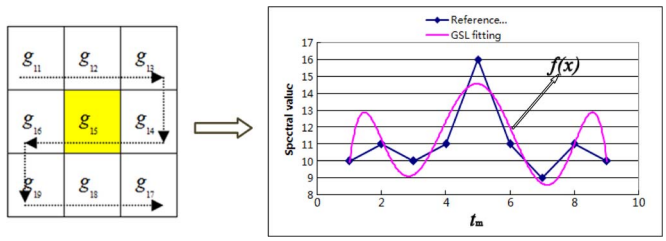

Fig. 2. Transformation of actual spectral values to a spectrum-trend curve.

N. m is a sequential number $m = \{1, 2, 3, \ldots, k\}$. $f'(t_m)$ is the derivative of $f(x)$ at $x = t_m = m \times (N/k)$. The derivative is a measure of how $f(x)$ changes as its input changes at x. Therefore, each element of T represents the ascendant or descendant trend at the corresponding position. Therefore, T could perform the trend of spectrum function $f(x)$ in a discrete manner.

In our study, a spectrum trend for a group of pixels within a local area (e.g., 3×3 sliding window) central at pixel (i,j) was formulated. The real spectral values within a sliding window were transformed into a serial data set by raster data encoding (row order) approach [22], as it is shown in Fig. 2. This discrete ordered data set was considered to fit the spectrum function $f(x)$ by GLS curve fitting technique. The ordered set can be defined as $P_1 = [p_{11}, p_{12}, p_{13}, \ldots, p_{1m}]$, where p_{1m} denotes the value corresponding to the serial order m. If the size of the sliding window is $n \times n$ pixels, then $m = g \times n + h$, where $i - \lfloor (n-1/2) \rfloor \le g \le i + \lfloor (n-1/2) \rfloor$, $j - \lfloor (n-1/2) \rfloor \le h \le j + \lfloor (n-1/2) \rfloor$. (g,h) is the position within a sliding window. Under this condition, the spectrum trend, which is represented by P_1, can be calculated by (1). An example is shown in Fig. 2. The actual spectral values within a 3×3 window are transformed into a spectrum function $f(x)$, and then, the spectrum trend can be given quantitatively by (1).

Compared with actual spectral values for detecting change from multitemporal images, spectrum trend is relatively more robust. It is well known that multitemporal images for CD are usually different in radiation, and the difference is caused by different atmospheric conditions, solar angles, soil moisture, etc. For an area within the current sliding window, its overall trend of spectrum will not be changed by a small variation of spectra value.

B. Calculation of Spectrum-Trend Similarity

After determining the suitable spectrum-trend calculation approach, the spectrum trend for each pixel in the image can be evaluated. The spectrum-trend similarity between windows on two date images of the same geographic area should be measured to formulate the change magnitude image. Let $T_1 = (f'_1(t_1), f'_1(t_2), f'_1(t_3), \ldots, f'_1(t_m))$ and $T_2 = (f'_2(t_1), f'_2(t_2), f'_2(t_3), \ldots, f'_2(t_m))$ be the corresponding spectrum trends of a central pixel and its neighboring pixel within a sliding window in two date images. The spectrum-trend similarity between T_1 and T_2 is measured as follows:

$$\Delta T = T_1 - T_2 = \begin{pmatrix} f'_1(t_1) - f'_2(t_1) \\ f'_1(t_2) - f'_2(t_2) \\ f'_1(t_3) - f'_2(t_3) \\ \vdots \\ f'_1(t_m) - f'_2(t_m) \end{pmatrix} \tag{2}$$

where ΔT includes the spectrum-trend change information between two date images for a central pixel, and the change magnitude $\|\Delta T\|$ is computed with

$$\|\Delta T\| = \sqrt{\sum_{m=1}^{k} (f_1'(t_m) - f_2'(t_m))^2} \tag{3}$$

where $\|\Delta T\|$ represents the spectrum-trend difference between the same center of the corresponding local areas in the two date images, which are normalized to [0, 255]. The greater $\|\Delta T\|$ is, the greater the difference between the paired spectrum trend within the same local geographic area is, and the higher the possibility of change is.

C. Threshold Determination for Binary CD Map

Threshold is an old question in CD method, and many threshold determination methods have been reported [23]. After preparing the change magnitude image, the CD method then generates the binary CD map. Threshold determination methods can be categorized into two: supervised and unsupervised [18]. In our study, an unsupervised threshold selection method called "OTSU" [24], which assumes that the change magnitude image to be threshold contains two classes of pixels or bimodal histogram (e.g., change and no change), then calculates the optimum threshold separating those two classes so that their combined spread (intraclass variance) is minimal. To verify the adaptability of the proposed approach, a classified method called "iterative self-organizing data analysis technique algorithm (ISODATA)" was also used to determine whether a pixel has changed or not in the following experiment.

III. Experiment

Two experiments were performed to test the feasibility and robustness of the proposed LSTS approach. The first experiment was designed to analyze the influence of the LSTS parameter window size (n). The second experiment was performed to compare the binary result of CD between different CD methods. Both experiments employed SPOT-5 images of Tianjin in different districts.

A. Experiment 1: LSTS Parameter

The first two data sets used in this experiment consist of RGB false color images acquired by the SPOT-5 satellite sensor in North China in years 2009 and 2010. The area selected for the experiment is a residential area. A section (476 × 355 pixels) of the two scenes has a spatial resolution of 2.5 m. Fig. 4(a) and (b) shows the years 2009 and 2010 images, respectively. Some blocks migrated in the two dates considered (see the bottom parts of the images). The available ground data lead to problems in accuracy assessment of the land-cover CD result. Fig. 4(c) shows the reference map, which is useful in accessing CD error. Such reference map was refined by manual analysis of the images considered. This experiment tested the different values of the LSTS parameter [window size (n)]. The degree of each sliding window polynomial function $f(x)$ was set to five, and $k = n \times n$.

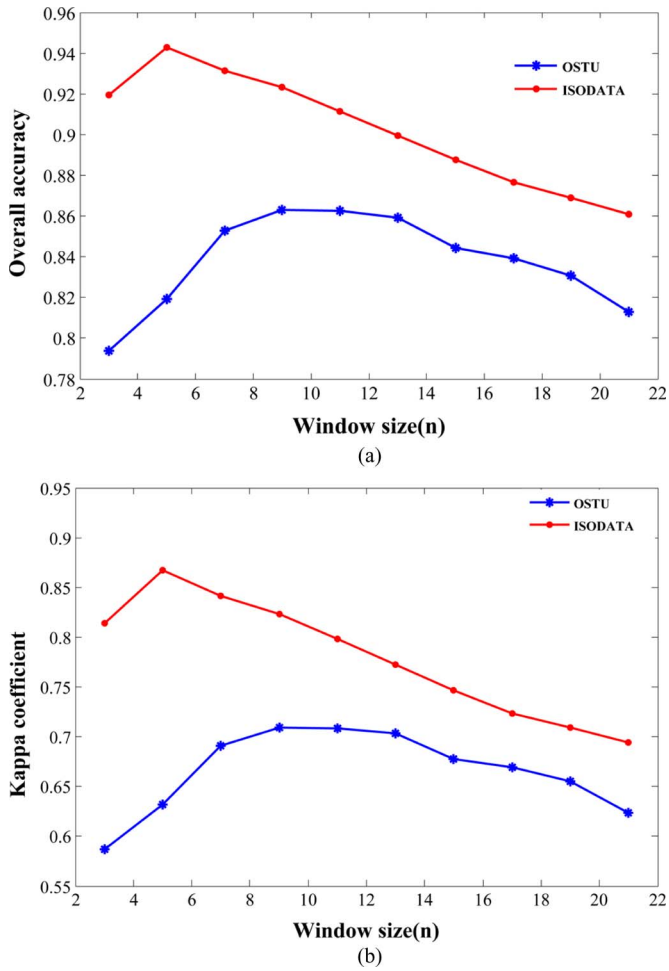

Fig. 3. Relationship between accuracy and window size (n) in different binary methods.

Parameter n, which indicates the maximum distance between the central pixel and its surrounding pixels, was considered to extract the spectrum trend. Selecting a suitable window size is the key to obtaining a highly accurate CD result because a window that is too small will provide detailed change information, whereas a window that is too large will remove noise but will introduce inaccurate change information. Fig. 3 shows that, when the value of n ranges from 3 to 21 for two different binary methods, the accuracy of the proposed approach increased first and then decreased. That is because, when the window size is large enough to obtain the optimum accuracy, the accuracy of each method decreases. Some visual results based on the threshold decision of OTSU are shown in Fig. 3. It can be seen from the result that a larger window will remove a lot of noise with the lost of change information and a smaller window provides detailed change information with a low accuracy. In this case study, when window size $= 5$, the proposed approach obtains its optimal performance with the threshold selection method OTSU [overall accuracy $(\mathrm{OA}) = 0.86$ and kappa coefficient $(\mathrm{Ka}) = 0.709$; see Fig. 4(g)].

B. Experiment 2: Accuracy Comparison of Different Methods

This experiment aims to compare the effectiveness of LSTS when different related CD methods are used. Another SPOT-5 image of Tianjin City was used. Fig. 5(a) and (b)

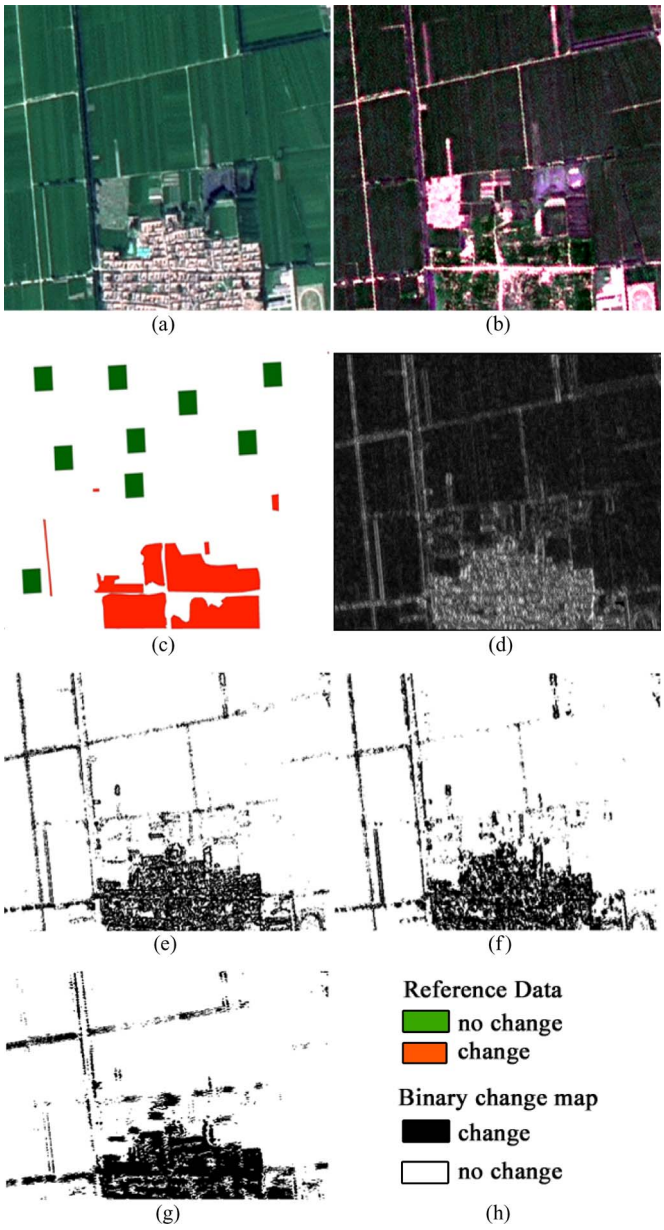

Fig. 4. Experiment images and some results using OTSU threshold decision. (a)–(c) T_1 image, T_2 image, and ground reference data. (d) Change magnitude image ($n = 5 \times 5$). (e) Binary map ($n = 3 \times 3$). (f) Binary map ($n = 5 \times 5$). (g) Binary map ($n = 9 \times 9$). (h) Legend for the reference data and binary result.

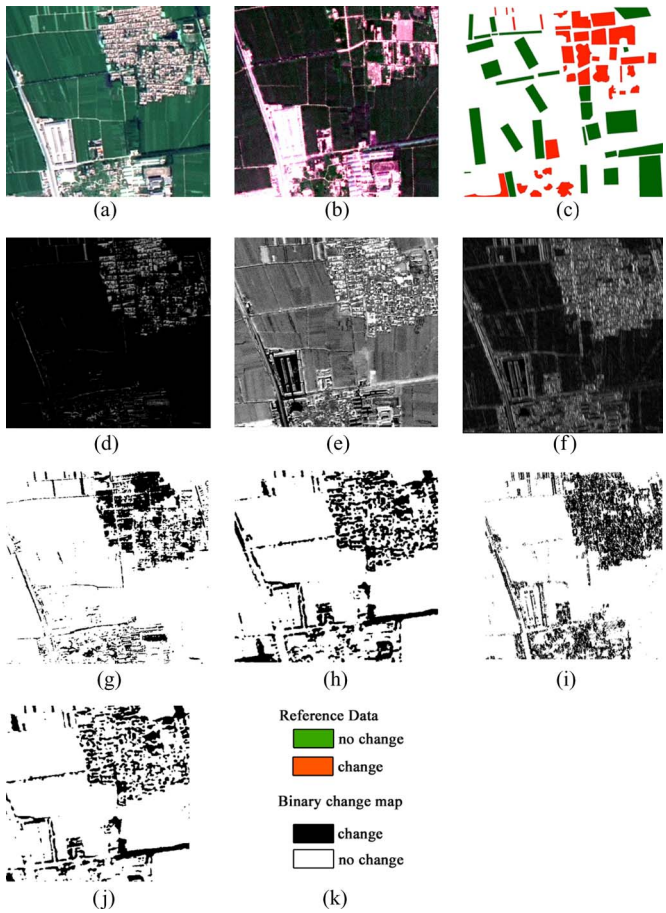

Fig. 5. Comparisons of different methods using OTSU threshold decision. (a)–(c) T_1 image, T_2 image, and ground reference data. (d)–(f) Change magnitude images for image difference, CVA, and LSTS approach. (g)–(j) Binary CM for image difference, CVA, LSTS approach, and method in [14]. (k) Legend.

TABLE I
CD RESULT FOR DIFFERENT METHODS ON THE BASIS OF THE ISODATA CLASSIFIER

Method	Overall Accuracy	Kappa
CVA	0.687	0.344
Image Difference	0.827	0.61
approach in [14]	0.71	0.33
LSTS	0.89	0.776

TABLE II
CD RESULT FOR DIFFERENT METHODS ON THE BASIS OF OTSU

Method	Overall Accuracy	Kappa
CVA	0.726	0.376
Image Difference	0.744	0.387
approach in [14]	0.71	0.33
LSTS	0.843	0.65

shows the images used (484 × 451 pixels), and Fig. 5(c) shows the ground reference data, which are collected manually by comparing the multitemporal images.

To evaluate the performance of the proposed LSTS approach, we compared the LSTS with three CD methods: image difference [1], traditional CVA [18], and PCA- and k-means-based approach [14]. To test the adaptability of the LSTS, the change magnitude image of each method was partitioned in the different methods: OTSU and ISODATA, respectively. A sliding window was utilized to extract spectrum trend for each pixel. The "change" versus "no-change" confusion matrix for each method was calculated by comparing the corresponding CD result with the same ground reference data. The results are illustrated in Tables I and II, respectively. When ISODATA is adopted as a classifier to partition the change magnitude image into a binary CD map (Table I), LSTS has a higher accuracy than other related methods in this case. Table II confirms this performance when another threshold selection method (OTSU) is used. Specially, LSTS is compared with the method in [14] in further experiments, and the results were shown in Table III.

IV. CONCLUSION

China has experienced tremendous land-cover changes in the urban areas. Therefore, a timely and accurate land-cover

TABLE III
ACCURACY COMPARISON BETWEEN LSTS AND APPROACH IN [14] WITH DIFFERENT WINDOW SIZES (n)

		n=3	n= 5	n = 7	n=9
Approach in[14]	OA	0.701	0.706	0.718	0.728
	Ka	0.314	0.330	0.369	0.399
LSTS	OA	0.821	0.843	0.848	0.853
	Ka	0.600	0.649	0.669	0.684

or land-use CD is extremely important to understand the relationships and interactions between humans and natural phenomena and to provide useful information for environmental protection, land planning, and decision making at the local, regional, national, and global levels. The proposed LSTS approach uses a sliding window to extract the spectrum trend for each central pixel to consider automatically the contextual information. Spectrum-trend similarity is employed instead of real spectral values to detect change.

LSTS is compared with different CD methods in two experiments by using SPOT-5 satellite images. On the basis of the performance of LSTS in experiment A, we can conclude that a large window will result in noise, whereas a small window will not contain enough spatial contextual information. In experiment B, the performance of LSTS is better than that of the image difference [1], traditional CVA [4], and PCA- and k-means-based approach [14]. When the overall accuracy and kappa coefficient are accessed, the quantitative assessments demonstrate that LSTS has higher accuracy in both experiments compared with the other CD methods. The application of LSTS in different binary methods demonstrates the adaptability of the proposed approach. The advantage of LSTS is that it supplies a feasible way of constructing the spectrum trend on the basis of the neighboring pixels. This approach is more effective than utilizing directly the real spectral value for binary land-cover CD.

LSTS exhibits good potential in binary land-cover CD. However, the proposed LSTS approach is simple in computation and technique, and the reliability of the proposed approach should be further evaluated. In addition, a suitable window size for extracting the spectrum trend is difficult to determine in applications and is time consuming. Therefore, LSTS should be improved, and the window size should be selected without manual intervention in future studies.

ACKNOWLEDGMENT

The authors would like to thank Prof. T. Celik, University of the Witwatersrand, for his friendly help in promoting the quality of our experiment.

REFERENCES

[1] A. Singh, "Review article digital change detection techniques using remotely-sensed data," *Int. J. Remote Sens.*, vol. 10, no. 6, pp. 989–1003, Jun. 1989.
[2] K. C. Tan, H. S. Lim, M. Z. MatJafri, and K. Abdullah, "Landsat data to evaluate urban expansion and determine land use/land cover changes in Penang Island, Malaysia," *Environ. Earth Sci.*, vol. 60, no. 7, pp. 1509–1521, Jun. 2010.
[3] T. Celik, "Multiscale change detection in multitemporal satellite images," *IEEE Geosci. Remote Sens. Lett.*, vol. 6, no. 4, pp. 820–824, Oct. 2009.
[4] J. Chen, P. Gong, C. He, R. Pu, and P. Shi, "Land-use/land-cover change detection using improved change-vector analysis," *Photogramm. Eng. Remote Sens.*, vol. 69, no. 4, pp. 369–380, Apr. 2003.
[5] J. Im and J. R. Jensen, "A change detection model based on neighborhood correlation image analysis and decision tree classification," *Remote Sens. Environ.*, vol. 99, no. 3, pp. 326–340, Nov. 2005.
[6] D. L. Corresponding, P. Mausel, E. Brondizio, and E. Moran, "Change detection techniques," *Int. J. Remote Sens.*, vol. 25, no. 12, pp. 2365–2401, Jun. 2004.
[7] M. Munsi, S. Malaviya, G. Oinam, and P. K. Joshi, "A landscape approach for quantifying land-use and land-cover change (1976–2006) in middle Himalaya," *Regional Environ. Change*, vol. 10, no. 2, pp. 145–155, Jun. 2010.
[8] R. S. Lunetta, J. F. Knight, J. Ediriwickrema, J. G. Lyon, and L. D. Worthy, "Land-cover change detection using multi-temporal MODIS NDVI data," *Remote Sens. Environ.*, vol. 105, no. 2, pp. 142–154, Nov. 2006.
[9] J. M. McHugh, J. Konrad, V. Saligrama, and P. M. Jodoin, "Foreground-adaptive background subtraction," *IEEE Signal Process. Lett.*, vol. 16, no. 5, pp. 390–393, May 2009.
[10] F. Bovolo and L. Bruzzone, "A theoretical framework for unsupervised change detection based on change vector analysis in the polar domain," *IEEE Trans. Geosci. Remote Sens.*, vol. 45, no. 1, pp. 218–236, Jan. 2007.
[11] C. He, A. Wei, P. Shi, Q. Zhang, and Y. Zhao, "Detecting land-use/land-cover change in rural-urban fringe areas using extended change-vector analysis," *Int. J. Appl. Earth Observ. Geoinf.*, vol. 13, no. 4, pp. 572–585, Aug. 2011.
[12] J. Chen, X. Chen, and X. Cui, "Change vector analysis in posterior probability space: A new method for land cover change detection," *IEEE Geosci. Remote Sens. Lett.*, vol. 8, no. 2, pp. 317–321, Mar. 2011.
[13] Y. Zhengwei and R. Mueller, "Spatial-spectral cross-correlation for change detection: A case study for citrus coverage change detection," in *Proc. ASPRS Annu. Conf.*, Tampa, FL, USA, 2007, vol. 5, pp. 7–11.
[14] T. Celik, "Unsupervised change detection in satellite images using principal component analysis and k-means," *IEEE Geoscience and Remote Sensing Letters*, vol. 6, no. 4, pp. 772–776, Oct. 2009.
[15] S. Z. Li, *Markov Random Field Modeling in Image Analysis*. New York, NY, USA: Springer-Verlag, 2009.
[16] L. Bruzzone and D. F. Prieto, "Automatic analysis of the difference image for unsupervised change detection," *IEEE Trans. Geosci. Remote Sens.*, vol. 38, no. 3, pp. 1171–1182, May 2000.
[17] T. Kasetkasem and P. Kumar Varshney, "An image change detection algorithm based on Markov random field models," *IEEE Trans. Geosci. Remote Sens.*, vol. 40, no. 8, pp. 1815–1823, Aug. 2002.
[18] J. F. Mas, "Monitoring land-cover changes: A comparison of change detection techniques," *Int. J. Remote Sens.*, vol. 20, no. 1, pp. 139–152, Jan. 1999.
[19] P. Sinha and L. Kumar, "Binary images in seasonal land-cover change identification: A comparative study in parts of New South Wales, Australia," *Int. J. Remote Sens.*, vol. 34, no. 6, pp. 2162–2186, Mar. 2013.
[20] Y. Yang, Y. Xia, F. Ge, Y. Meng, and H. Yu, "A trend based similarity calculation approach for mining time series data," in *Proc. Int. MultiConf. Eng. Comput. Sci.*, 2012, vol. 1, pp. 461–464.
[21] H. Gu and G. Rong, "Evaluate time delay from sensor's data by trend similarity search," *Int. J. Syst. Sci.*, vol. 40, no. 12, pp. 1307–1317, Dec. 2009.
[22] F. Holroyd and S. Bell, "Raster GIS: Models of raster encoding," *Comput. Geosci.*, vol. 18, no. 4, pp. 419–426, May 1992.
[23] P. Rosin, "Thresholding for change detection," in *Proc. 6th Int. Conf. Comput. Vis.*, 1998, pp. 274–279.
[24] N. Otsu, "A threshold selection method from gray-level histograms," *IEEE Trans. Syst., Man, Cybern.*, vol. SMC-9, no. 1, pp. 62–66, Jan. 1979.